AIP Applied Physics Letters

Stress-mediated magnetic anisotropy and magnetoelastic coupling in epitaxial multiferroic PbTiO3-CoFe2O4 nanostructures

C. Y. Tsai, H. R. Chen, F. C. Chang, W. C. Tsai, H. M. Cheng, Y. H. Chu, C. H. Lai, and W. F. Hsieh

Citation: Applied Physics Letters **102**, 132905 (2013); doi: 10.1063/1.4800069
View online: http://dx.doi.org/10.1063/1.4800069
View Table of Contents: http://scitation.aip.org/content/aip/journal/apl/102/13?ver=pdfcov
Published by the AIP Publishing

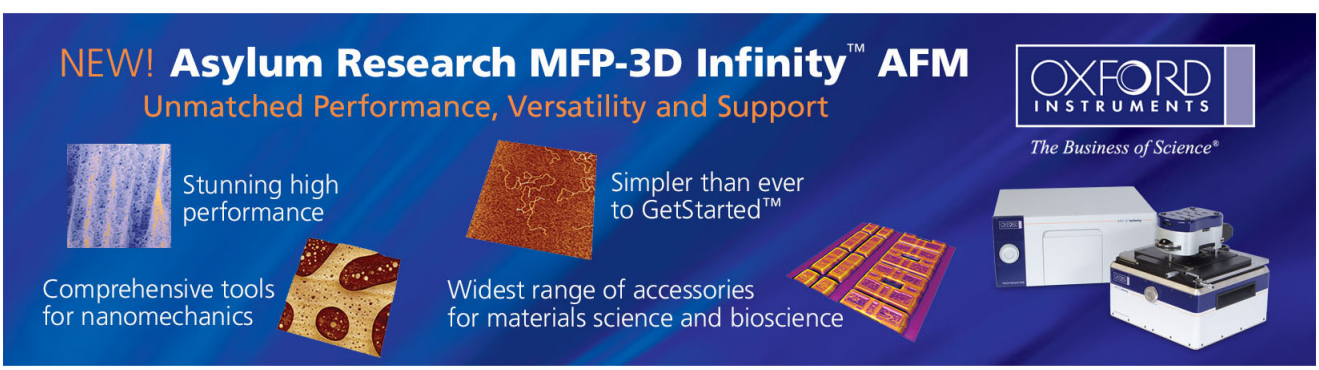

Stress-mediated magnetic anisotropy and magnetoelastic coupling in epitaxial multiferroic $PbTiO_3$-$CoFe_2O_4$ nanostructures

C. Y. Tsai,[1] H. R. Chen,[1] F. C. Chang,[2,3] W. C. Tsai,[4] H. M. Cheng,[3] Y. H. Chu,[2] C. H. Lai,[4] and W. F. Hsieh[1,a)]

[1]*Department of Photonics and Institute of Electro-Optical Engineering, National Chiao Tung University, 1001 Tahsueh Rd., Hsinchu 300, Taiwan*
[2]*Department of Materials Science and Engineering, National Chiao Tung University, Hsinchu 31040, Taiwan*
[3]*Material and Chemical Research Laboratories, Industrial Technology Research Institute, Hsinchu 310, Taiwan*
[4]*Department of Materials Science and Engineering, National Tsing Hua University, Hsinchu 31013, Taiwan*

(Received 9 January 2013; accepted 22 March 2013; published online 5 April 2013)

This study reports a self-assembled multiferroic nanostructure, composed of $PbTiO_3$ (PTO) pillars embedded in a $CoFe_2O_4$ (CFO) matrix, deposited on MgO(001) by pulsed laser deposition. The epitaxial relationship in the PTO-CFO nanostructure is $(100)[101]_{PTO} \parallel (001)[101]_{CFO} \parallel (001)[101]_{MgO}$, confirming the in-plane aligned polarization of PTO. The perpendicular magnetic anisotropy of this thin film results from the magnetoelastic anisotropy that exceeds the shape anisotropy. The increased frequency and the enhanced intensity of the tetrahedral (T-) site phonon modes by increasing the magnetic field indicate strong magnetoelastic coupling through magnetostriction in this multiferroic nanostructure. The anisotropic Raman strength enhancement of the T-site phonon along different directions suggests the magnetoelastic coupling is most efficient in the in-plane direction. © *2013 American Institute of Physics*. [http://dx.doi.org/10.1063/1.4800069]

Multiferroic materials, distinguished as simultaneously possessing several ferroic orders, have attracted significant research interest because of their magnetoelectric (ME) coupling, which is the magnetic property modulated by an electric field or vice versa.[1] Self-assembled perovskite-spinel nanostructures such as $BaTiO_3$-$CoFe_2O_4$ (BTO-CFO),[1] $BiFeO_3$-$CoFe_2O_4$ (BFO-CFO),[2] and $PbTiO_3$-$CoFe_2O_4$ (PTO-CFO)[3] can improve room temperature (RT) ME coupling by mediating the efficient elastic stress at the perovskite-spinel interfaces.[4,5]

CFO is a promising candidate as a spinel phase in self-assembly multiferroics for providing the strong magnetostriction[6] to enhance ME coupling. The composition of the two phases,[7] the strain-states of these phases,[8,9] and the lattice parameters of substrates[9] all play important roles in manipulating the magnetic properties of CFO nanostructures. Recent research has shown that the out-of-plane magnetic anisotropy results from the out-of-plane compressive stress on CFO in low-temperature fabricated BTO-CFO system[8] and in less spinel-phase constituted BFO-CFO system.[7] As for PTO-CFO on $SrTiO_3$(001), prior studies have shown that the in-plane magnetic anisotropy is due to the out-of-plane tensile stress on CFO.[2,10] Moreover, because of the sensitivity to crystal symmetry and short range ordering,[11,12] phonons can be used as local probes for detecting the strains of a BFO-CFO nanostructure[13] and the magnetoelastic coupling in $PbZrTiO_3$(PZT)-CFO bi-layer materials through magnetic-field-dependent Raman scattering.[14] However, the magnetic field affected phonon dynamics in self-assembled nanostructures, and the magnetic anisotropy of PTO-CFO nanostructures[10,15,16] have rarely been reported.

Therefore, the aim of this study is to provide more insight into the magnetic anisotropy and phonon evolution of PTO-CFO nanostructures based on magnetostriction. This study shows that PTO-CFO on MgO(001) simultaneously exhibits in-plane piezoelectric properties and out-of-plane magnetic anisotropy. The strongly enhanced and hardened T-site phonons after increasing the magnetic field are the result of increased compressive stress driven by the magnetostriction.

The PTO-CFO thin film was deposited by pulsed laser deposition (PLD, KrF laser) using a composite target of $(CoFe_2O_4)_2$-$(PbTiO_3)_1$ at 600 °C under the oxygen pressure of 100 mTorr. The structural and piezoelectric properties of the thin film were characterized by an x-ray diffractometer (HRXRD, Bede D1) with *Cu*-$k_{\alpha 1}$ radiation and piezoelectric force microscopy (PFM, Veeco Escope AFM) with an ac voltage of 4 V, respectively. We measured the magnetic properties with a vibrating sample magnetometer (VSM) at RT. Micro-Raman spectra were recorded using a LabRam Jobin-Yvon spectrometer equipped with the liquid nitrogen-cooled CCD and 532 nm excitation. Before measuring the magnetic-field-dependent Raman scattering, the thin film was demagnetized. The laser spot was kept at the same position as applying the magnetic field.

Figure 1(a) shows the θ-2θ x-ray diffraction pattern along the surface normal. The diffraction peaks of PTO(100), PTO(200), and CFO(004) confirm the well-crystallized thin film on MgO(001) without other intermediate phases. The sharp full width at half maximum (FWHM) of 0.008° for CFO(004) in the inset shows that the CFO has good quality, whereas a broad FWHM of 1.528° for PTO implies a high strain or more than one domain. To understand the effect of MgO substrate ($a = 4.21$ Å) on the strain states of PTO-CFO, we calculated the lattice constants from

a)Author to whom correspondence should be addressed. Electronic mail: wfhsieh@mail.nctu.edu.tw

the XRD measurements. The calculated lattice constants of CFO (bulk, $a = 8.38$ Å) are $a = b = 8.397$ Å and $c = 8.358$ Å, and those of PTO (bulk, $a = 3.9$ Å and $c = 4.15$ Å) are $a = b = 3.954$ Å and $c = 4.001$ Å. The strain on CFO relaxes more ($\varepsilon_{001} = -0.263\%$ and $\varepsilon_{100} = 0.131\%$) on MgO than on other substrates, such as $SrTiO_3$ (Ref. 8) and $MgAl_2O_4$ (Ref. 17) because of lattice compatibility. The tetragonalities (c/a) of CFO and PTO are 0.995 and 1.012, respectively. Although the c/a of PTO decreases as compared with the bulk PTO, PTO still has a tetragonal structure with ferroelectric and piezoelectric properties. The ϕ-scan across the PTO(101), CFO(202), and MgO(202) shown in Fig. 1(b) confirms that this thin film adopts a four-fold symmetry and exhibits the epitaxial relationship of $(100)[101]_{PTO} \parallel (001)[101]_{CFO} \parallel (001)[101]_{MgO}$. The c-axis of PTO orients in the in-plane direction, differing from the polar axes of the self-assembly multiferroics on $SrTiO_3(001)$.[2,4,18]

We performed PFM measurement to detect the ferroelectric domains and identify the distribution of the two phases. The AFM topography in Fig. 2(a) shows a uniform morphology with an average grain size of 110 nm and the small roughness of approximately 4 nm. Figures 2(b) and 2(c), respectively, show the phase and the combination of amplitude and phase signals for the in-plane PFM. The absence of the out-of-plane PFM signal indicates the thin film contains only a-domains. The bright and dark regions, respectively, labeled as "A" and "B" in Fig. 2(b) represent opposite polarizations. Conversely, the middle color region with no PFM response should be referred to CFO phases. The random distribution of a-domains in the image indicates PTO pillars are embedded in the CFO matrix. The a_2-domains with the polarization direction perpendicular to that of a_1-domains (Fig. 2(c)) were recorded in Fig. 2(d) after a sample rotation of 90°. The angle-resolved PFM[19] shows that this nanostructure contains two horizontal polar domains in accordance with the broad FWHM of the PTO(100) diffraction peak. The percentages of a_1-domains and a_2-domains are approximately 20% and 15% that leads to a total coverage ratio of approximately 35%, consisting with the molar ratio of the target. The in-plane polarization of a PTO-CFO multiferroic on MgO(001) offers an in-plane electric field for manipulating magnetic properties and vice versa.

The magnetic hysteresis loops in Fig. 3 show different magnetization behaviors along the in-plane (dotted line) and out-of-plane (circle line) directions. A comparable small magnetic field of approximately 15 kOe is enough to saturate the magnetic moments of the sample. The coercive field (H_C) along the in-plane direction (210 Oe) is much smaller than that along the out-of-plane direction (2280 Oe). The shrinkage of the in-plane H_C implies that the spin has more than one preferred orientation. Because CFO is a strong magnetostrictive material, the stress imposed on the thin film can change the magnetic properties of CFO. We estimated the ratio of remanence to saturation magnetization[20] (Mr/Ms) to be 42.9% and 16.0% for applying magnetic field along the out-of-plane and in-plane directions, respectively. The results show that the easy-axis is along the out-of-plane direction.

The magnetic anisotropy of nanostructures is based on their magnetoelastic anisotropy and shape anisotropy. Because CFO functions as a matrix rather than a rod, its shape anisotropy should contribute to an in-plane spin orientation instead of an out-of-plane spin orientation. By adopting a 2D model[21] for the thin film, the estimated shape anisotropy of $-2\pi M_S^2$ is -0.772×10^5 J/m^3. However, the vertical compressive stress and the biaxial tensile stress generate magnetoelastic anisotropy in the out-of-plane direction. The calculated magnetoelastic energy of $K_{me} = -3/2\lambda_{33}(C_{11}-C_{12})(\varepsilon_{100}-\varepsilon_{001})$ is 6.75×10^5 J/m^3, where λ_{33} is the

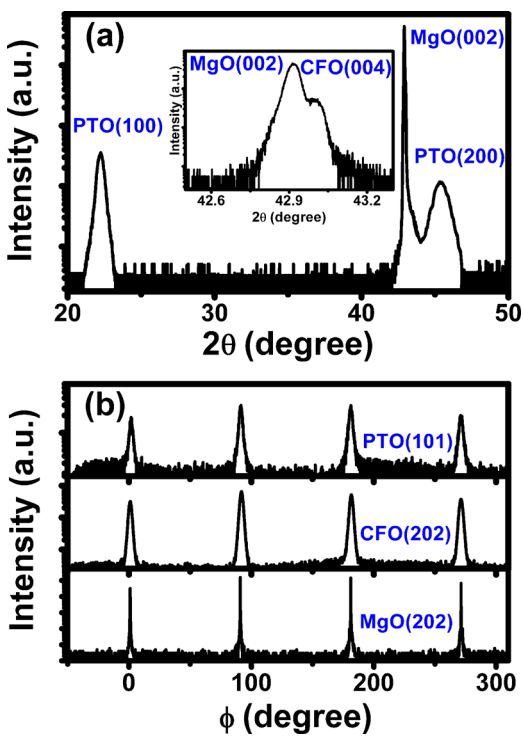

FIG. 1. (a) XRD θ-2θ scan along surface normal with a magnification of CFO(004) in the inset and (b) the ϕ−scan profiles across PTO{101}, CFO{202}, and MgO{202} off-normal reflections, respectively.

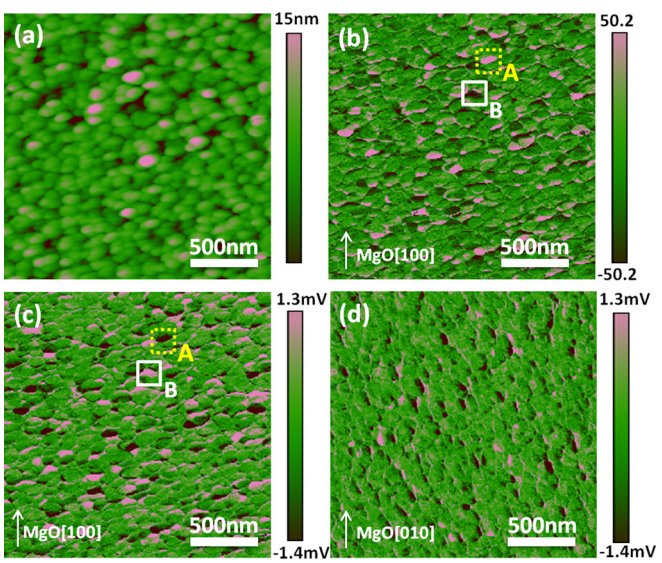

FIG. 2. (a) The AFM showing the surface morphology, (b) the IP-PFM (in-plane) phase images where the bright and dark colors, respectively, marked as "A" and "B" represent opposite polarizations, (c) the corresponding IP-PFM image combined with the phase and amplitude signals, and (d) the IP-PFM image taken after rotating the sample perpendicular to the direction of Fig. 2(b).

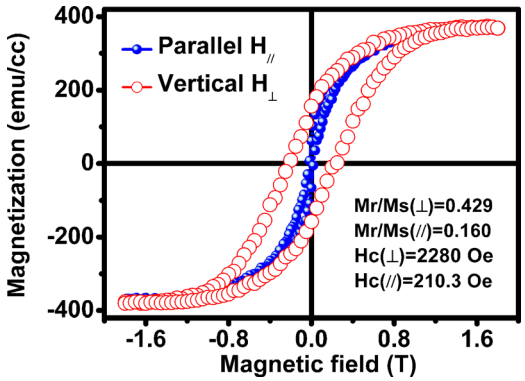

FIG. 3. The magnetic hysteresis loops with the applied magnetic fields along the out-of-plane direction (red circle) and along the in-plane direction (blue dot), respectively.

magnetostriction coefficient of -590×10^{-6}, and C_{11} and C_{12} are the elastic constants of 2.7×10^{12} and 1.06×10^{12} dyn/cm^2, respectively.[7,21] Therefore, the total anisotropy energy prefers a vertical spin orientation because the magnetoelastic energy exceeds the shape anisotropy. The biaxial tensile stress from the substrate tunes the magnetic anisotropy of this thin film to the out-of-plane direction. The result differs from the in-plane magnetic easy-axis in PTO-CFO on $SrTiO_3$(001).[2,10]

We further investigated the local strain states of the sample using micro-Raman scattering. Comparing the Raman spectrum of PTO-CFO with those of the pure CFO and PTO thin films at the bottom of Fig. 4(a), a broad peak at 300 cm^{-1} is attributed to the superposition of the $B_1 + E$ and A_1(2TO) modes of PTO and the E_g mode of CFO. The peak at 500 cm^{-1} originates from a combination of the E(3TO) mode of PTO and the T_{2g}(3) mode of CFO. Although these modes overlap, other phonons at lower and higher frequencies can be investigated recognizably.

PTO with a tetragonal structure adopts the P4*mm* space group yielding $3A_1 + 3E$ and $B_1 + E$ modes at RT.[22] According to the appearance of the *a*-domains and the absence of the *c*-domains in PTO, the A_1(TO), E(TO), and $B_1 + E$ modes are allowed in a geometry with backscattering configuration along the substrate normal.[22] The stress analysis of pure PTO thin film is generally based on the E(TO) modes because they are not affected by the domain structures.[23] However, the E(TO) modes of PTO overlap with the phonons of CFO in this nanostructure. Therefore, we only discussed the A_1(TO) phonons. The soft mode A_1(1TO) at approximately 100 cm^{-1} of the nanostructure is broader and weaker because PTO is highly strained. The red-shifting of A_1(1TO) gives an estimated stress of 4 GPa on PTO.[24] A high-frequency A_1(3TO) phonon should shift approximately 70 cm^{-1} according to the Curie-Weiss pressure law[24,25] as indicated by the dotted-line in the spectra. Therefore, the mode near 550 cm^{-1} represents A_1(3TO), which is consistent with the predicted value.

For a tetragonal symmetry of $CoFe_2O_4$ spinel, $I4_1/amd$ space group analysis yields 10 Raman modes of $2A_{1g} + 3B_{1g} + B_{2g} + 4E_g$.[26,27] The Raman modes with frequencies lower than 500 cm^{-1}, labeled as O-site phonons, represent the bending of oxygen toward the metals in octahedral sites (BO_6). The A_{1g}(1) (700 cm^{-1}) and A_{1g}(2) (625 cm^{-1}) modes,

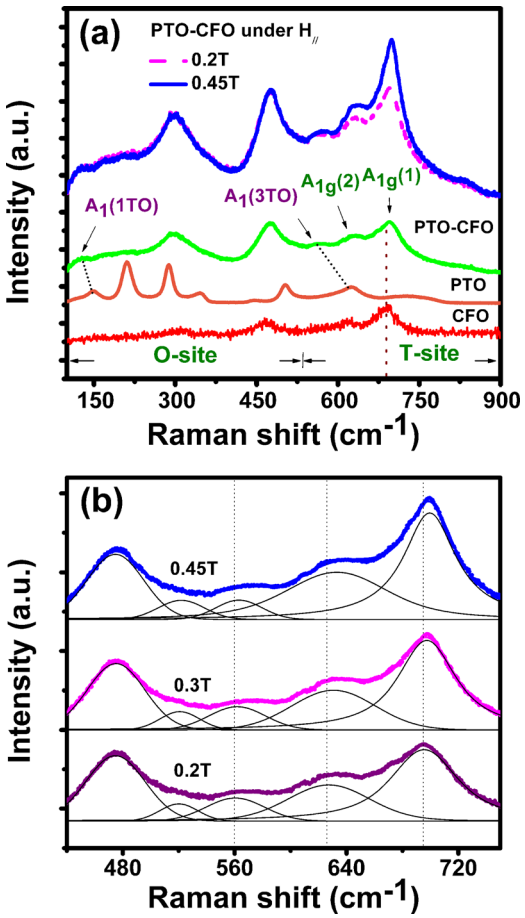

FIG. 4. (a) The Raman spectra of PTO-CFO thin film under the in-plane magnetic fields of 0 T (green line), 0.2 T (pink dot), and 0.45 T (blue line), respectively. The pure CFO (red) thin film and pure PTO thin film (orange) are shown at the bottom of this figure as references; (b) the fitted Raman spectra of PTO-CFO nanostructure under the in-plane magnetic fields of 0.2 T, 0.3 T, and 0.45 T, respectively.

labeled as T-site phonons, represent the stretching of the surrounding oxygen against tetrahedral metals (AO_4).[27] The T-sites in the partial inverse spinel structure, such as $CoFe_2O_4$, are occupied by Fe^{3+} and partial Co^{2+}, depending on the inversion parameter.[28] The blue-shifted T-site phonon of PTO-CFO in comparison with that of pure CFO thin film shows the compressively strained CFO in PTO-CFO. Conversely, the red-shifted phonon frequencies of BFO-CFO show the tensile stress.[13]

Figure 4(a) shows the phonon evolutions under the in-plane magnetic fields of 0.2 T (pink dotted line) and 0.45 T (blue solid line), respectively. The O-site modes retain almost the same frequencies and show little decrease in intensity as the magnetic field increases. By normalizing the intensity of the T-site phonons to the O-site phonon at 470 cm^{-1}, we found strong enhancements of T-site phonons as the magnetic field increases from 0.2 T to 0.45 T, especially the A_{1g}(1) mode at approximately 700 cm^{-1}. Because the T-site phonons show more magnetic-field related properties than the O-site phonons, the magnetic field should disturb the local structural environments more in the T-sites than in the O-sites.

The fitted Raman spectra in Fig. 4(b) show that the frequency of the A_{1g}(1) phonon shifts toward 695.4 cm^{-1},

697.5 cm^{-1}, and 699.5 cm^{-1} under applied magnetic fields of 0.2 T, 0.3 T, and 0.45 T, respectively. Another T-site phonon, the $A_{1g}(2)$ mode, shifts from 627.4 cm^{-1} to 633.1 cm^{-1} as the magnetic field increases from 0.2 T to 0.45 T. Figures 5(a) and 5(b) show the fitted phonon frequency and the intensity, respectively. The origin of phonon softening or hardening under magnetic fields is correlated with the spin-phonon coupling[29] or the magnetostriction[14] of $CoFe_2O_4$. The T-site and O-site phonons are softer in CFO particles because of the spin-phonon coupling caused by the increased magnetic ordering under an applied magnetic field.[29] Therefore, the magnetostriction dominates the T-site phonon hardening in PTO-CFO.

The magnetostriction of a multiferroic material is correlated with the changes of phonon frequency. The $A_{1g}(1)$ mode is attributed to the Fe-O stretching vibrations of the FeO_4 tetrahedra along the {111} directions, and its frequency follows[12] $w_0 \sim \frac{1}{(a_0^2+b_0^2+c_0^2)^{3/2}}$, where a_0, b_0, and c_0 are the lattice constants of CFO. According to the magnetostriction, the lattice constant of CFO becomes shorter (or longer) under a parallel (or perpendicular) magnetic field taking account of the negative (or positive) magnetostrictive coefficient λ_{33} (λ_{13}) of -590×10^{-6} (110×10^{-6}).[20] The mode frequency, which depends on the lattice constants, changes because of the magnetostriction. Therefore, the variation of the T-site mode frequency under the magnetic field can be derived as $w_{(H)} \sim w_0 \times \frac{(a_0^2+b_0^2+c_0^2)^{3/2}}{(a_1^2+b_1^2+c_1^2)^{3/2}}$, where the changes of lattice constants a_1, b_1, and c_1 are $(\lambda_{33}+1)a_0$, $(\lambda_{13}+1)b_0$, and $(\lambda_{13}+1)c_0$, respectively, under an external magnetic field applied along the a_0 axis. Although the phonon shift of 4 cm^{-1} in our experimental results exceeds the predicted value (less than 1 cm^{-1}) under a magnetic field of 0.45 T, the experimental value is close to the variation of the T-site phonons in a bi-layer multiferroic PZT/CFO under a magnetic field of 0.28 T.[14] This slight difference implies that magnetostriction is even larger in a micro-scale range than a long-range order. In addition, the initial strain states of CFO vary the magnitudes of magnetostrictive coefficients.[30]

The compressive stress generated by the magnetic field on the thin film results in the phonon hardening and should alter the local electron configuration as well.[20] The in-plane compressive stress and out-of-plane tensile stress distort the local metal-oxygen bonding, making it more asymmetric for both T-site and O-site phonons. Because of the shorter distance between the tetrahedral metal and the surrounding oxygen, the T-site phonon should be more sensitive to configuration variations than the O-site phonon with a larger atomic distance. Therefore, distorted tetrahedral bonding induces a different Raman scattering cross-section as the observed enhancement in the T-site phonon intensity.

We performed similar experiments by applying the magnetic field along the out-of-plane direction (Figs. 5(a) and 5(b)) and found the enhancement of the T-site phonon intensity is smaller than that under an in-plane magnetic field. The phonon shift seems to become saturated under a lower out-of-plane magnetic field. The different behaviors of magnetostriction along different directions could result from the initial strain states of CFO. Recent research has shown that the magnetostrictive coefficient (λ_{33}) of CFO decreases when a strain gauge is applied parallel to the magnetic field.[30] The applied magnetic field at maximal magnetostriction also decreases as the strain increases.[30] Because the CFO is out-of-plane compressed in the proposed multiferroic material, the magnetostriction along the surface normal is reduced and more easily saturated. Therefore, the anisotropic phonon Raman strength enhancement under different magnetic field directions is correlated with anisotropic strain conditions through a stress-mediated process. In conclusion, the magnetic field induced T-site phonon hardening in this study confirms that magnetoelastic coupling is possible through magnetostriction. Anisotropic Raman strength enhancement of T-site phonon illustrates the in-plane direction is an efficient coupling direction in PTO-CFO nanostructure that could be concerned for the design of multiferroic devices.

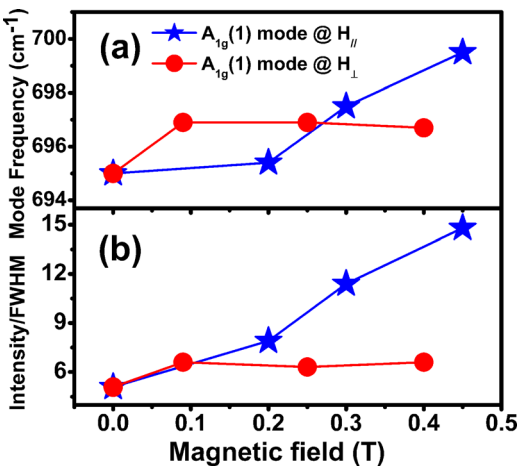

FIG. 5. The variations of frequency (a) and the intensity (b) of the $A_{1g}(1)$ mode under the magnetic fields applied along the in-plane (blue star) and the out-of-plane (red circle) directions.

This work was partially supported by National Science Council of Taiwan under Grant Nos. NSC-99-2112-M-009-009-MY3 and NSC 99-2221-E-009-095-MY3.

[1]H. Zheng, J. Wang, S. E. Lofland, Z. Ma, L. Mohaddes-Ardabili, T. Zhao, L. Salamanca-Riba, S. R. Shinde, S. B. Ogale, F. Bai, D. Viehland, Y. Jia, D. G. Schlom, M. Wuttig, A. Roytburd, and R. Ramesh, Science **303**, 661 (2004).
[2]N. Dix, R. Muralidharan, J.-M. Rebled, S. Estradé, F. Peiró, M. Varela, J. Fontcuberta, and F. Sánchez, ACS Nano **4**, 4955 (2010).
[3]I. Levin, J. Li, J. Slutsker, and A. Roytburd, Adv. Mater. **18**, 2044 (2006).
[4]F. Zavaliche, H. Zheng, L. Mohaddes-Ardabili, S. Y. Yang, Q. Zhan, P. Shafer, E. Reilly, R. Chopdekar, Y. Jia, P. Wright, D. G. Schlom, Y. Suzuki, and R. Ramesh, Nano Lett. **5**, 1793 (2005).
[5]L. W. Martin, S. P. Crane, Y.-H. Chu, M. B. Holcomb, M. Gajek, M. Huijben, C.-H. Yang, N. Balke, and R. Ramesh, J. Phys.: Condens. Matter **20**, 434220 (2008).
[6]D. Fritsch and C. Ederer, Phys. Rev. B **86**, 014406 (2012).
[7]N. M. Aimon, D. H. Kim, H. K. Choi, and C. A. Ross, Appl. Phys. Lett. **100**, 092901 (2012).
[8]H. Zheng, J. Kreisel, Y. H. Chu, R. Ramesh, and L. Salamanca-Riba, Appl. Phys. Lett. **90**, 113113 (2007).
[9]R. Comes, M. Khokhlov, H. Liu, J. Lu, and S. A. Wolf, J. Appl. Phys. **111**, 07D914 (2012).
[10]J. Li, "Engineering of self-assembled multiferroic nanostructures in $PbTiO_3$-$CoFe_2O_4$ thin films," Ph.D. dissertation (University of Maryland, 2006), pp. 46–47.
[11]V. G. Ivanov, M. V. Abrashev, M. N. Iliev, M. M. Gospodinov, J. Meen, and M. I. Aroyo, Phys. Rev. B **82**, 024104 (2010).
[12]M. N. Iliev, D. Mazumdar, J. X. Ma, A. Gupta, F. Rigato, and J. Fontcuberta, Phys. Rev. B **83**, 014108 (2011).

[13]O. Chaix-Pluchery, C. Cochard, P. Jadhav, J. Kreisel, N. Dix, F. Sánchez, and J. Fontcuberta, Appl. Phys. Lett. **99**, 072901 (2011).
[14]Z. Li, Y. Wang, Y. Lin, and C. Nan, Phys. Rev. B **79**, 180406(R) (2009).
[15]M. Murakami, K.-S. Chang, M. A. Aronova, C.-L. Lin, M. H. Yu, J. H. Simpers, M. Wuttig, I. Takeuchi, C. Gao, B. Hu, S. E. Lofland, L. A. Knauss, and L. A. Bendersky, Appl. Phys. Lett. **87**, 112901 (2005).
[16]M. Pan, Y. Liu, G. Bai, S. Hong, V. P. Dravid, and A. K. Petford-Long, J. Appl. Phys. **110**, 034103 (2011).
[17]I. Stern, J. He, X. Zhou, P. Silwal, L. Miao, J. M. Vargas, L. Spinu, and D. H. Kim, Appl. Phys. Lett. **99**, 082908 (2011).
[18]Z. P. Tan, A. L. Roytburd, I. Levin, K. Seal, B. J. Rodriguez, S. Jesse, S. Kalinin, and A. Baddorf, Appl. Phys. Lett. **93**, 074101 (2008).
[19]M. Park, S. Hong, J. Kim, J. Hong, and K. No, Appl. Phys. Lett. **99**, 142909 (2011).
[20]B. D. Cullity and C. D. Graham, *Introduction to Magnetic Materials*, 2nd ed. (Wiley, Hoboken, NJ, 2009).
[21]A. Lisfi, C. M. Williams, L. T. Nguyen, J. C. Lodder, A. Coleman, H. Corcoran, A. Hohnson, P. Chang, A. Kumar, and W. Morgan, Phys. Rev. B **76**, 054405 (2007).
[22]A. Bartasyte, O. Chaix-Pluchery, J. Kreisel, J. Santiso, M. Boudard, C. Jimenez, A. Abrutis, and F. Weiss, IEEE Trans. Ultrason. Ferroelectr. Freq. Control **54**, 2623 (2007).
[23]A. Bartasyte, S. Margueron, J. Santiso, J. Hlinka, E. Simon, I. Gregora, O. Chaix-Pluchery, J. Kreisel, C. Jimenez, F. Weiss, V. Kubilius, and A. Abrutis, Phase Trans. **84**, 509 (2011).
[24]P.-E. Janolin, P. Bouvier, J. Kreisel, P. A. Thomas, I. A. Kornev, L. Bellaiche, W. Crichton, M. Hanfland, and W. Crichton, Phys. Rev. Lett. **101**, 237601 (2008).
[25]J. A. Sanjurjo, E. López-Cruz, and G. Burns, Phys. Rev. B **28**, 7260 (1983).
[26]P. Chandramohan, M. P. Srinivasan, S. Velmurugan, and S. V. Narasimhan, J. Solid State Chem. **184**, 89 (2011).
[27]Z. W. Wang, R. T. Downs, V. Pischedda, R. Shetty, S. K. Saxena, C. S. Zha, Y. S. Zhao, D. Schiferl, and A. Waskowska, Phys. Rev. B **68**, 094101 (2003).
[28]J. A. Moyer, D. P. Kumah, C. A. Vaz, D. A. Arena, and V. E. Henrich, Appl. Phys. Lett. **101**, 021907 (2012).
[29]T. Yu, Z. X. Shen, Y. Shi, and J. Ding, J. Phys.: Condens. Matter **14**, L613 (2002).
[30]A. Muhammad, R. S. Turtelli, M. Kriegisch, R. Grossinger, F. Kubel, and T. Konegger, J. Appl. Phys. **111**, 013918 (2012).